

## HIFIRE DIRECT-CONNECT RIG (HDCR) PHASE I GROUND TEST RESULTS FROM THE NASA LANGLEY ARC-HEATED SCRAMJET TEST FACILITY

Neal Hass and Karen Cabell  
NASA Langley Research Center  
Hampton, VA

Andrea Storch  
ATK Space Systems, NASA Langley Research Center  
Hampton, VA

### ABSTRACT

The initial phase of hydrocarbon-fueled ground tests supporting Flight 2 of the Hypersonic International Flight Research Experiment (HIFiRE) Program has been conducted in the NASA Langley Arc-Heated Scramjet Test Facility (AHSTF). The HIFiRE Program, an Air Force-lead international cooperative program includes eight different flight test experiments designed to target specific challenges of hypersonic flight. The second of the eight planned flight experiments is a hydrocarbon-fueled scramjet flight test intended to demonstrate dual-mode to scramjet-mode operation and verify the scramjet performance prediction and design tools. A performance goal is the achievement of a combusted fuel equivalence ratio greater than 0.7 while in scramjet mode. The ground test rig, designated the HIFiRE Direct Connect Rig (HDCR), is a full-scale, heat sink, direct-connect ground test article that duplicates both the flowpath lines and the instrumentation layout of the isolator and combustor portion of the flight test hardware. The primary objectives of the HDCR Phase I tests are to verify the operability of the HIFiRE isolator/combustor across the Mach 6.0 – 8.0 flight regime and to establish a fuel distribution schedule to ensure a successful mode transition prior to the HiFiRE payload Critical Design Review. Although the phase I test plans include testing over the Mach 6 to 8 flight simulation range, only Mach 6 testing will be reported in this paper. Experimental results presented here include flowpath surface pressure, temperature, and heat flux distributions that demonstrate the operation of the flowpath over a small range of test conditions around the nominal Mach 6 simulation, as well as a range of fuel equivalence ratios and fuel injection distributions. Both ethylene and a mixture of ethylene and methane (planned for flight) were tested. Maximum back pressure and flameholding limits, as well as a baseline fuel schedule, that covers the Mach 5.84 – 6.5 test space have been identified.

### NOMENCLATURE

|                    |   |
|--------------------|---|
| $M_0$              | = flight Mach number  |
| $q_0$              | = flight dynamic pressure (psf)                                   |
| $M_2$              | = isolator entrance Mach number                                   |
| $P_2$              | = isolator entrance static pressure (psia)                        |
| $H_{t2}$           | = isolator entrance total enthalpy (Btu/lbm)                      |
| $P_{t,pl}$         | = facility plenum stagnation pressure (psia)                      |
| $H_{t,pl}$         | = facility plenum enthalpy (Btu/lbm)                              |
| $\phi$             | = fuel equivalence ratio  |
| $\phi(\text{pri})$ | = fuel equivalence ratio injected at primary injection station    |
| $\phi(\text{sec})$ | = fuel equivalence ratio injected at secondary injection station  |
| $\phi(\text{tot})$ | = total equivalence ratio = $\phi(\text{pri}) + \phi(\text{sec})$ |
| $\phi_b$           | = total fuel equivalence ratio burned                             |
| $x$                | = axial distance from isolator entrance (in)                      |

## Acronyms

|        |   |
|--------|---|
| AFRL   | = Air Force Research Laboratories                     |
| AHSTF  | = Arc-Heated Scramjet Test Facility                   |
| BS     | = Body side (Top)                                     |
| CS     | = Cowl side (Bottom)                                  |
| DSTO   | = Australian Defense and Science Technology Office    |
| HDCR   | = HIFiRE Direct Connect Rig                           |
| HF2    | = HIFiRE Flight 2                                     |
| HIFiRE | = Hypersonic International Flight Research Experiment |
| TBC    | = thermal barrier coating                             |
| TDLAS  | = Tuneable Diode Laser Absorption System              |

## INTRODUCTION

The Hypersonic International Flight Research and Experimentation (HIFiRE) Program is a bi-lateral collaboration executed by an integrated team representing the U.S. Air Force Research Laboratory (AFRL) and the Australian Defense Science and Technology Organization (DSTO). Further, the US Air Force has secured a Space Act Agreement with NASA to advance the collaborative development and demonstration of hypersonic aero-propulsion technologies. The objective of the HIFiRE Program is to increase understanding of fundamental hypersonic phenomena and to develop technologies deemed critical to the realization of next generation aerospace vehicles. The purpose is to extend the hypersonic database and enhance the accuracy of complex models and simulations. Phenomena will be examined and characterized at flight conditions that are difficult, if not impossible, to model with current computational methods and/or simulate in ground test facilities. The product of this program is an experimental flight laboratory to capture extensive coherent high-fidelity data. The scope of this program encompasses a series of 8 focused research projects<sup>1</sup>.

The HIFiRE Flight 2 (HF2) scramjet experiment is planned to explore the operating, performance, and stability characteristics of a simple hydrocarbon-fueled scramjet combustor as it transitions from dual-mode to scramjet-mode operation and during supersonic combustion at Mach 8+ flight conditions.<sup>2</sup> Dual mode operation is characterized by large-scale flow separation, significant regions of subsonic combusting flow and combustion-induced pressure rise upstream of the primary fuel injection site. Scramjet-mode operation is characterized by supersonic combusting flow with no large scale flow separation and minimal combustion-induced pressure rise upstream of the primary fuel injection site. A fuel mixture composed of ethylene and methane will be used as a surrogate for thermally stressed JP-7<sup>3</sup>.

There are several objectives of the HF2 flight test experiment. The primary objectives are the successful operation of a hydrocarbon fueled scramjet combustor at a burned fuel equivalence ratio ( $\phi_{ib}$ ) greater than 0.7 at enthalpies equal to or greater than Mach 8, and the verification of performance prediction tools. Additional objectives include 1) the successful transition from dual-mode to scramjet-mode operation with which to verify the mode transition prediction capability, 2) the evaluation of a gaseous fuel mixture as a surrogate for cracked liquid hydrocarbon fuel, 3) demonstration of a flight test approach that provides a variable Mach number flight corridor at nearly constant dynamic pressure, and 4) the verification of the AFRL Tuneable Diode Laser Absorption System (TDLAS) for combustion performance determination.

The development of the HF2 scramjet experiment has matured and at present has nearly completed its design cycle. Before releasing the design for manufacturing, some level of confidence that the experiment will be successful must be demonstrated by means other than computational analyses. The HIFiRE Direct-Connect Rig (HDCR) is a ground test model that was constructed to verify the HIFiRE F2 flowpath design and demonstrate that a range of operability, with margin, is achievable. The results of the Mach 6 tests conducted to date are presented in this report and demonstrate that the flowpath design has the margin necessary for successful dual-mode operations.

## HIFiRE FLIGHT 2 MISSION DESCRIPTION

A Pedro-Oriole two-stage sounding rocket, similar to the HYSHOT<sup>4</sup> two-stage Terrier-Orion shown in Figure 1, will be used to ferry the payload to the initial test condition and through the test condition window. A centerline cut of the preliminary payload design is shown in Figure 2. The shroud encapsulates and protects the inlet during the boost to test conditions. At the selected conditions, gas bags force a separation of the shroud into two pieces which then deploy from the payload. The forebody is made up of opposing 7-degree ramps that extend back to the sidewalls of the rectangular 1 inch high by 4.8 inch wide inlet.<sup>5</sup> A boundary layer trip strip, located 15 inches downstream of the forebody leading edge, ensures a turbulent boundary layer to mitigate the risk of boundary layer separations due to incident shocks. An inlet with an internal contraction ratio of 1.2 further compresses the flow. From the isolator entrance (point A), the flowpath extends down the center of the payload until the end of the combustor expansion section (point B). Aft of the combustor, the flow is split with a bifurcating nozzle, clocked 90 degrees from forebody ramps, that vent the flow outward and overboard.



Figure 1. HYSHOT launch vehicle assembly.

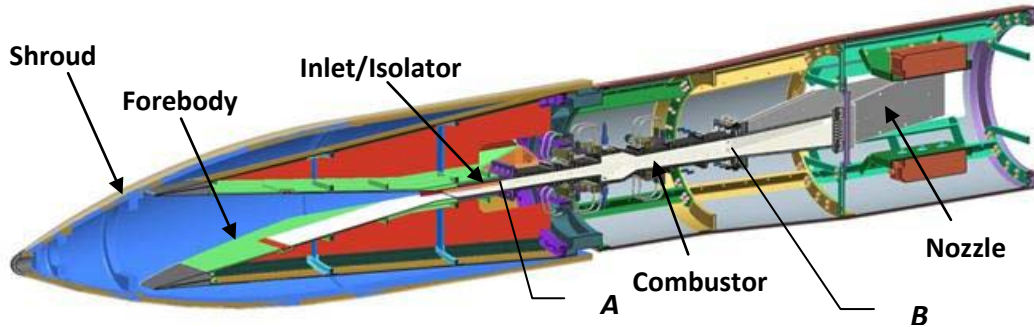


Figure 2. HF2 scramjet experiment payload centerline cut.

Unlike typical sounding rocket trajectories, the HF2 will delay second stage ignition, and after a sustained coast while experiencing a 1-g pitchover, the second stage will fire at an attitude, determined from Monte-Carlo trajectory analyses, that will accelerate the payload through the test window. Figure 3 shows the nominal trajectory on an altitude versus Mach number plot. Preliminary results of the Monte-Carlo studies indicated the 2-sigma dispersion of trajectory solutions falls within the 1000-3000 psf range of dynamic pressures. The lines of constant dynamic pressure at these extremes establish the operability limits of the experiment.

The experiment begins with a shroud separation event at the Mach 5.2 condition. After a brief tare event, the fueling commences at Mach 5.8. After light-off, a stabilization period will occur lasting 1-2 seconds. Then, the fuel will be injected according to a set fuel equivalence ratio schedule with the prescribed distribution, or “fuel split” among the various injection sites. As the payload accelerates, it is desired that the changing flight test conditions drive the mode transition, as opposed to the varying fuel distribution. This simplifies the post flight analysis by reducing the number of variables that change at each point analyzed in the trajectory. Therefore, the fuel split is to be held constant through the dual-mode to scramjet-mode transition, and throughout the remaining scramjet portion of the test window.

## GROUND TEST GOALS AND OBJECTIVES

The goals of the HDCR ground test experiment are 1) to verify that the isolator/combustor portion of the HIFiRE flowpath design demonstrates satisfactory operability with margin, using the surrogate fuel, spanning the engine transition from dual-mode to scramjet operation, across the flight test trajectory window and 2) to provide data to support analytical tools verification.

A number of objectives were identified for the HDCR tests in order to meet the verification requirements for the flight test flowpath. These objectives include 1) determination of the requirement for, and number of, spark ignitors, 2) determination of fuel injector port sizing, 3) determination of the sensitivity to fuel type and fuel temperature, 4) identification of fuel splits for ignition (with margin to prevent unstart), for transition from dual-mode to scramjet-mode, and for scramjet operation at  $\phi_b > 0.7$ . A final objective is to obtain a data set for use in verifying the performance prediction tools.

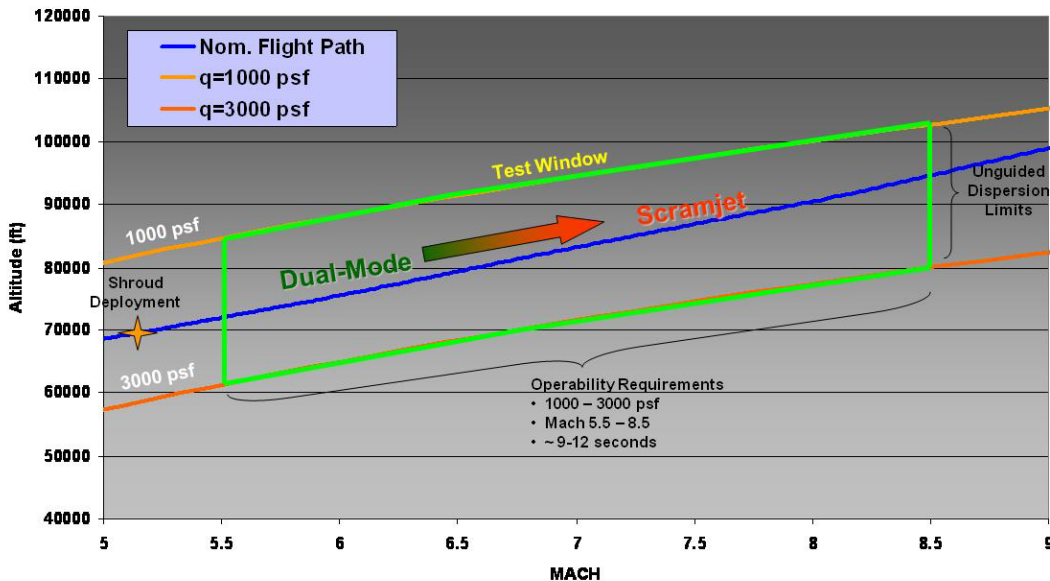


Figure 3. HF2 Nominal Trajectory.

### TEST APPROACH

Exclusion of the flight flowpath inlet and nozzle from the ground test model enabled a full-scale isolator and combustor test article to be installed and tested in NASA Langley's Arc-Heated Scramjet Test Facility (AHSTF) in a direct-connect test mode. The parameters that map the direct-connect ground test conditions to flight conditions are the inlet exit/ isolator entrance Mach number ( $M_2$ ), static pressure ( $P_2$ ), and the stagnation enthalpy ( $H_{t2}$ ). It is not possible to simulate the continuous flight trajectory with a fixed-geometry facility nozzle. So, to capture sufficient data in the ground test, three facility nozzles were designed to have exit Mach numbers matching the isolator entrance Mach numbers calculated for Mach 6, 7 and 8 flight conditions. The nozzles are thus referred to nominally as the Mach 6, 7, and 8 facility nozzles. The facility stagnation pressure is adjusted to provide facility nozzle exit static pressure matching the flight isolator entrance static pressure and the facility stagnation enthalpy is adjusted to match the flight isolator entrance stagnation enthalpy. Both the stagnation pressure and enthalpy can be adjusted independently to investigate the sensitivity of the engine operation to pressure and temperature. Other parametric variation capability includes: fuel distribution, fuel temperature and fuel equivalence ratio. The fuel temperature parametric capability was not exercised in this phase, but will be in future testing.

The facility generates the isolator entrance flow properties corresponding to the conditions generated by the aerodynamic processing of the flight payload inlet, but only in a one-dimensional sense. Flow distortion characteristics, resulting from the flight forebody and inlet compression process, are not simulated in the HDCR ground test. Some of the flow features not matched to flight in the HDCR testing include: reflected shocks from the forebody/inlet processing, boundary layer thickness, surface temperatures, and ingested air composition. The incoming boundary layer of the ground test article is significantly thinner than that generated by the flight inlet. In addition the wall temperature history will be

different between ground and flight due to different heating time histories. These factors will further contribute to boundary layer effects and heat loss that are not flight-like. Another non-flight like aspect of the ground test is the presence of nitric oxide in the test gas as a result of arc-heating the air. Although the nitric oxide reduces the available oxygen content of the incoming air stream, studies have shown that under certain conditions nitric oxide can enhance combustion.<sup>6,7,8</sup> The reduction of available oxygen causes the fuel equivalence ratio to be slightly higher than atmospheric air with 21% molar oxygen. For the results reported in this paper, no correction for nitric oxide content is made and the fuel equivalence ratio is calculated assuming the test gas has a molar composition of 21% oxygen, 78% nitrogen and 1% Argon.

## TEST HARDWARE DESCRIPTION

### FACILITY DESCRIPTION

The AHSTF has historically been used for free-jet testing of air-frame integrated scramjet engine models.<sup>9,10</sup> However, the HDCR flowpath is directly coupled to one of the three facility nozzles designed to simulate the flight isolator entrance conditions. Thus, the HDCR tests are the first use of the facility in direct-connect mode.

A schematic of the facility is shown in Figure 4. A portion of the air is heated by an electric arc and then mixed with unheated bypass air in a plenum chamber to achieve a desired mixture stagnation enthalpy. The total mixed air stream is then expanded through the facility nozzle. Each of the three HDCR nozzles has a rectangular cross-section with a 1 inch high x 4 inch wide exit to match the HDCR isolator flowpath entrance. The test gas passes through the engine flowpath where fuel is injected for combustion and the resulting gas exhausts into the 4-ft diameter test section. The flow is then diffused to subsonic velocity, cooled by an after-cooler and exhausted into four 60-ft diameter vacuum spheres connected in series.

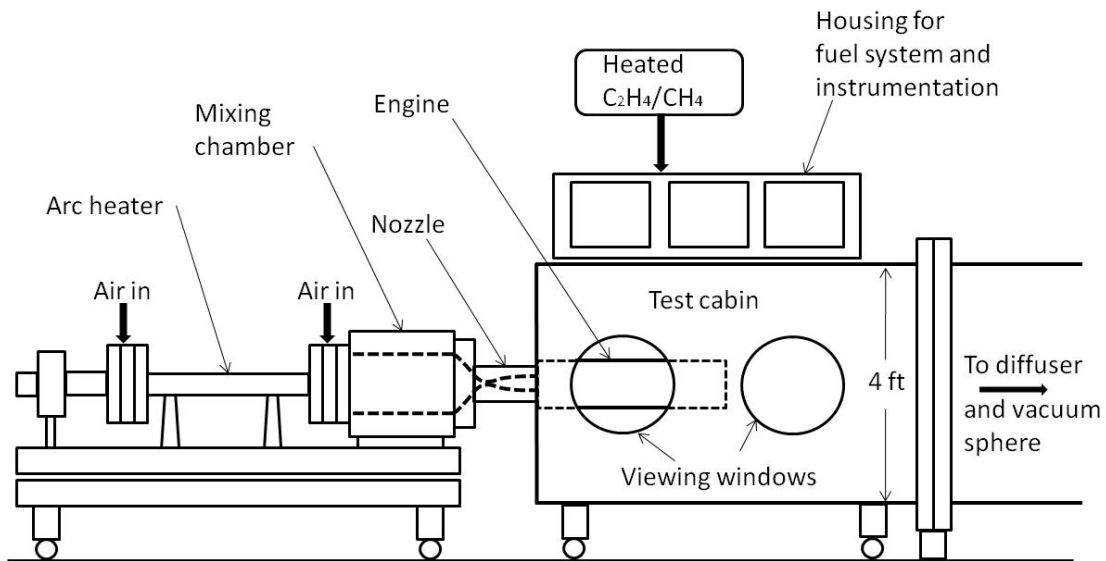


Figure 4. Facility schematic.

The AHSTF fuel delivery system, previously capable of delivering only ambient temperature hydrogen and silane, was modified to deliver gaseous hydrocarbon fuels. The fuel selected for the HIFIRE flight experiment as well as the HDCR ground tests is a 64%-36% (molar) ethylene-methane mixture which serves as a surrogate for thermally stressed JP-7. Testing was initiated with pure ethylene because of the experience base with ethylene both from a fuel delivery standpoint and a scramjet combustion standpoint. Ethylene was used in shakedown testing and in a majority of the tests at Mach 6. Heating the fuel upstream of expansion processes in the system (i.e. across regulators and flow control valves) was necessary to prevent liquification of the ethylene (critical temperature of 49F compared to the methane critical temperature of -117F, and the mixture critical temperature of 11F).

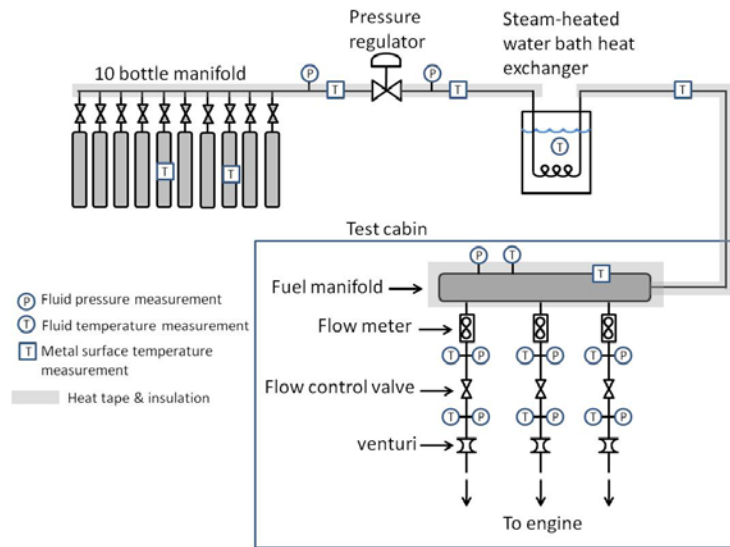


Figure 5. Simplified schematic of HDCR fuel system.

A simplified schematic of the fuel delivery system is shown in Figure 5. Fuel is supplied from a rack of 10 k-bottles manifolded together. Each bottle is wrapped in a heating jacket to warm the fuel upstream of the expansion across the regulator, which regulates from the bottle pressure (maximum of 2000 psia) to the desired test cabin pressure (typically 400 to 800 psia). Downstream of the regulator is a steam-heated water-bath heat exchanger to heat the fuel upstream of the test cabin, where the fuel is expanded again across flow control valves. Heat tape and insulation are installed on all the piping from the 10-bottle manifold up to and including the test cabin manifold to prevent heat loss. All the heating systems' (bottle warmers, heat tape, and water bath) temperatures are thermostatically controlled.

From the test cabin manifold, there are three separate legs to independently fuel three injection stations on the engine. Each leg has a control valve to control fuel flow rate to each station. The fuel flow rate is calculated via a sonic flow equation using stagnation pressure and temperature measurements upstream of a calibrated sonic venturi. This flow rate is used in closed-loop control of the valve position. There is also a volume flow meter and close-coupled pressure and temperature measurement in each leg for an independent calculation of the flow rate. Fuel equivalence ratios quoted in the results use the venturi derived mass flow. Both types of flow rate calculation (sonic venturi or flow meter) require thermodynamic modeling of the fuel to compute either the sonic mass flux (for the venturi calculation) or the density (for the flow meter calculation). Both the mass flux and density were computed via curve fits developed from data provided in the NIST software, REFPROP<sup>11</sup>.

A typical test sequence is shown below in Figure 6. Total test time from tunnel start-up to beginning of shut-down is anywhere from 20 to 30 seconds, mostly depending on the duration of the engine fueling sequence. Tunnel start-up and the establishment of “steady” conditions in the facility plenum chamber requires 12 to 15 seconds. This is followed by a 2 second engine tare and the execution of the fuel sequence. Three to four tests were typically conducted per run day.

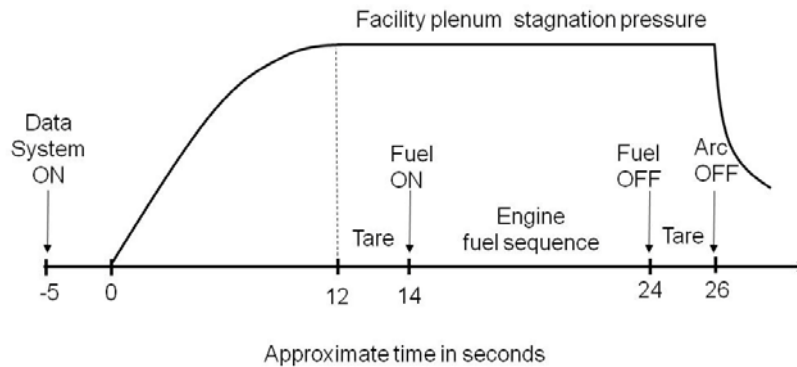


Figure 6. Typical HDCR run timeline.

Data was acquired at 10 Hz with the AHSTF’s dedicated data acquisition system which includes a Neff 500/600 system with 192 general purpose analog to digital channels and an Esterline electronically scanned pressure (ESP) 8400 system with 512 channels which was used for measuring flowpath surface pressures. Both the Neff and the Esterline systems were controlled with a Pentium PC running Autonet data acquisition software.

### RIG DESCRIPTION

Views of the HDCR test rig are shown in Figure 7. The rig is manufactured from Oxygen-free High Conductivity® (OFHC) copper with wall thicknesses of 2.0 inches. The flowpath inner mold lines are shown in Figure 8 with the key transition geometry points included<sup>12</sup>. The HDCR test rig duplicates the flowpath of the flight test payload from point A to point B in Figure 2. The flowpath width is constant at 4 inches. The overall length of the HDCR is 28.0 inches with an isolator entrance height of 1.0 inch, and a combustor exit height of 1.908 inches. The flowpath surfaces are coated with a 0.025 inch thick zirconia thermal barrier coating (TBC) to extend the maximum run time and cycle life of the rig. Information on the development of the flowpath inner mold lines can be found in reference 12.



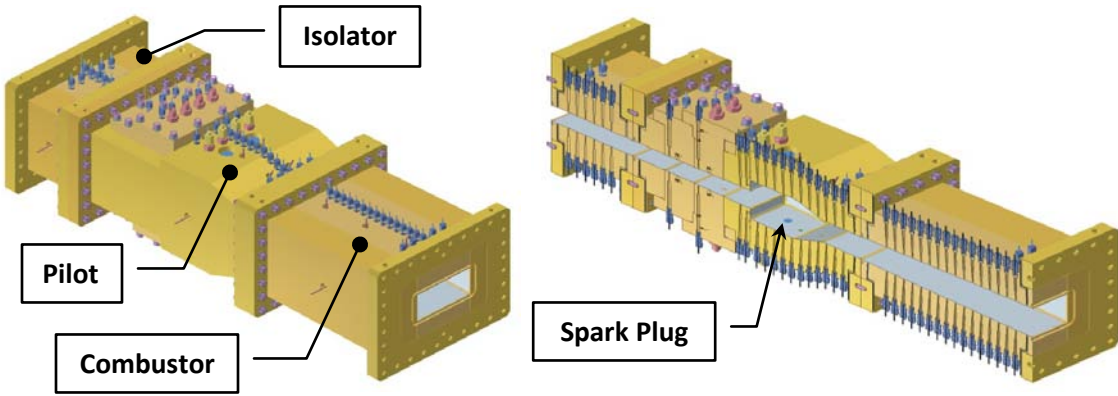


Figure 7. HDCR rig with centerline cut view.

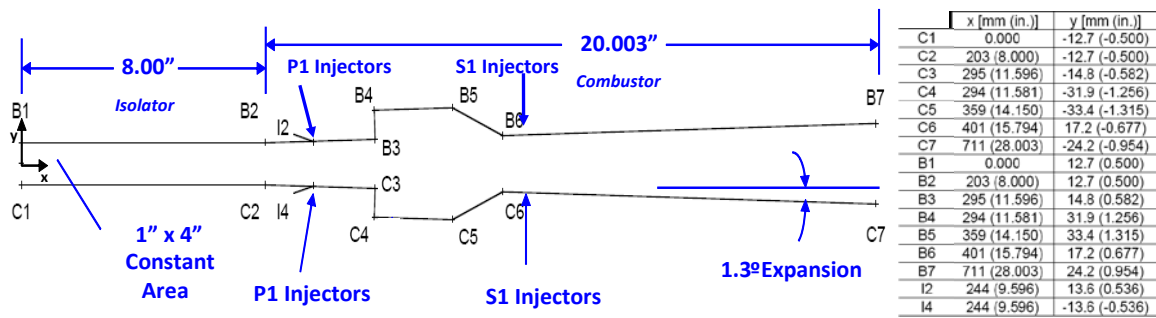


Figure 8. HDCR inner mold lines.

Five injector stations were built into the model as a parametric feature, but only the P1 injectors ( $x=9.59$  inches) and S1 injectors ( $x=16.5$  inches) were employed for the Mach 6 tests. For the remainder of this report, the P1 injectors are referred to as the primary injectors (denoted as “pri” or “P”), and the S1 injectors are referred to as the secondary injectors (denoted as “sec” or “S”). At each axial injection station there are four injector holes on the bodyside, fed from a dedicated fuel manifold, and four injector holes on the cowl side, fed from a separate dedicated manifold, for a total of eight injection holes per station. Each injector hole is spaced equally across the width of the flowpath. The injector holes on the body side directly oppose those on the cowl side. The primary injectors are 0.125 inch diameter bores which are canted 15 degrees downstream off the wall. The secondary injectors are 0.094 inch diameter straight through ports that provide normal injection.

The results presented in this report cover several different injector configurations. The baseline injector configuration is the 4x4 which describes the use of all four injectors, both body side and cowl side at both the primary and secondary injector stations. In this configuration, and at the dual-mode operating conditions, the injectors operate unchoked. (Note: The design intent is to operate with choked injectors. The unchoked operating condition resulted from a change made to the flight inlet, reducing air capture, that occurred after the HDCR was manufactured). To explore the effect of penetration and mixing on the performance, injector ports can be disconnected and capped. Two other configurations tested were 2x2-I, which describes use of only the two inboard injectors on both body and cowl side, and the 2x2-O which describes use of only the two outboard injector pairs. The two specific 2x2 combinations tested were 2x2-I at both primary and secondary (denoted 2x2 P-I/S-I) and 2x2-I at the primary with 2x2-O at the

secondary (denoted 2x2 P-I/S-O). For the 2x2 configurations, the injectors were choked. A final modification tested in the 4x4 configuration included the installation of choked orifices at the flare fittings upstream of the injector ports. This was to ensure a uniform lateral fuel distribution, which was questionable for unchoked injectors. This configuration is denoted with the letter “C” in subsequent tables and figures.

Four spark ignitors are located within the cavity, two on the body side, and two on the cowl side, just downstream of the cavity injection ports. These are identified in by the blue circle within the flowpath shown in Figure 7. Spark ignitors could be turned on or off as needed to test for auto-ignition.

The HDCR rig has the same instrumentation layout as the flight test payload to ensure a direct comparison of results from flight to ground. The instrumentation consisted of static pressure ports, heat flux gauges, and thermocouples. The layout of the instrumentation is shown in Figure 9. The blue circles indicate the locations of static pressure ports, the red diamonds indicate the locations of the thermocouples, and the ‘X’ boxes indicate the locations of the heat flux gauges.

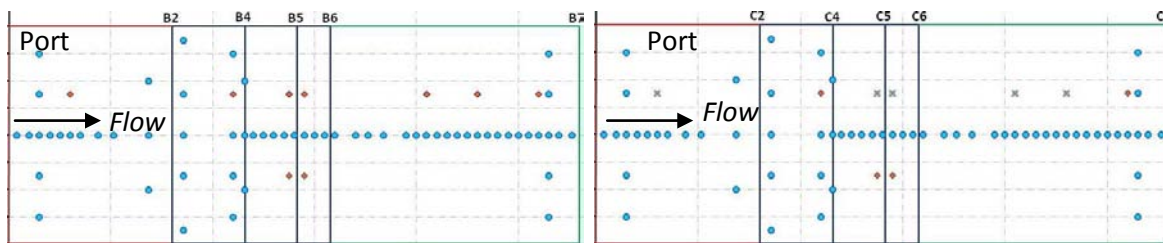


Figure 9a. Bodyside instrumentation layout.

Figure 9b. Cowlside instrumentation layout.

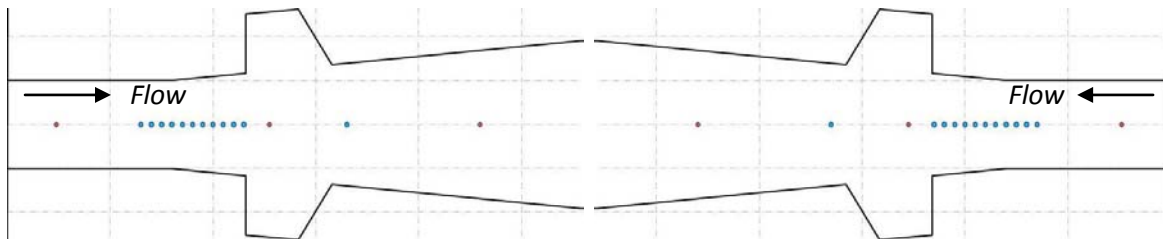


Figure 9c. Port side instrumentation layout.

Figure 9d. Starboard side instrumentation layout.

The rig contains 144 static pressure ports, 19 flowpath surface thermocouples, and 4 heat flux gauges. The pressure ports are 0.04” in diameter and connected to ESP modules having ranges of 45, 100, 250, and 750 psia. Centerline ports were spaced at 0.5” intervals where possible. Spanwise ports are located at the 1.5”, 6.9”, 8.6”, 11”, and 26.5” axial stations, both body and cowl side.

Flowpath surface thermocouples are located at axial stations 3”, 11”, 13.75”, 14.5”, 20.5”, 23”, and 26.5” along the flowpath, 0.75” off-centerline towards the starboard, to give clearance from the centerline pressure ports. The body side thermocouples were zirconia TBC coated and the cowlside thermocouples were left bare in order to assess thermal loads modeling with TBC coated hardware. To assist in accomplishing this assessment, the thermocouples were located at the same axial and off-centerline locations, but opposing each other. The process interpreting the TBC coated thermocouple measurements is described in a companion paper given at this conference<sup>13</sup>. There were also two port

and two starboard sidewall thermocouples centered vertically, and located at axial stations 12.75" and 23" to assess heat loads to the sidewalls.

The heat flux gauges are located on the cowl side only, at the same axial stations as the thermocouples, and 0.75" off-centerline to the port side of the flowpath. This was done intentionally to compare the heat loads measured to that extracted from thermocouple data. All the units were a Medtherm water-cooled model with a 500 BTU/ft<sup>2</sup>-s range. None of the heat flux gauges were TBC coated. The use of this data, and how to relate it to modeling the heat loads, is described in detail in reference 13.

### TEST CONDITIONS AND FLIGHT SIMULATION

Only Mach 6 facility nozzle testing is reported herein. Mach 6 testing was conducted first due to the need to have the fuel light-off characterized and the operability margin relative to unstart and flameout identified. Table 1 summarizes the test conditions and flight conditions simulated with the Mach 6 nozzle.  $H_{t,pl}$  and  $P_{t,pl}$  are the facility plenum stagnation enthalpy and pressure, respectively.  $M_o$  is the simulated flight Mach number corresponding to the stagnation enthalpy and  $q_o$  is the simulated flight dynamic pressure. In addition to matching the isolator entrance geometry, the HDCR simulation objective was to match the 1-dimensionalized isolator entrance Mach number, static pressure, and stagnation enthalpy predicted by flight CFD. Defining a flight simulation begins with identifying the facility nozzle exit, or isolator entrance Mach number, because it uniquely defines the flight Mach number and thus the target point in the trajectory. The exit Mach number and static-to-total pressure ratio were computed using results of CFD analysis of the as-designed facility nozzle geometry with a small correction applied to account for as-built versus as-designed differences. Results of flight inlet CFD analysis<sup>14</sup> at Mach 6, 7 and 8 were then used to determine the flight Mach number that would yield a one-dimensionalized throat Mach number equal to the computed facility nozzle exit Mach number. For the Mach 6 nozzle, the computed exit Mach number is 2.55 and the corresponding flight Mach number is 5.84. Corresponding values of the target one-dimensionalized throat static pressure and stagnation enthalpy are also obtained from the flight CFD results.

**Table 1. HDCR Test Conditions with the Mach 6 nozzle; Nozzle exit Mach = 2.55.**

| Condition     | $H_{t,pl}$<br>(Btu/lbm) | $P_{t,pl}$<br>(psia) | $M_o$ | $q_o$<br>(psf) |
|---------------|-------------------------|----------------------|-------|----------------|
| 6a – baseline | 719                     | 212                  | 5.84  | 1060           |
| 6b            | 719                     | 275                  | 5.84  | 1370           |
| 6c            | 719                     | 318                  | 5.84  | 1575           |
| 6d            | 873                     | 212                  | 6.50  | --             |

The facility typically duplicated stagnation enthalpy within three percent of the target throat stagnation enthalpy. However, all tests were conducted at reduced pressure compared to flight, due to instrumentation thermal limits. The simulated freestream dynamic pressures quoted in the table were determined by scaling the target flight dynamic pressure (corresponding to the simulated flight Mach number) by the ratio of actual to target isolator entrance pressure. The actual isolator entrance pressure was determined from the facility stagnation pressure and the facility nozzle exit static-to-total pressure ratio.

Condition 6a in table 1 represents the baseline flight simulation for the Mach 6 nozzle. Conditions 6b and 6c are dynamic pressure excursions from the baseline conditions. Condition 6d is an excursion from the baseline which was conducted to investigate engine operability over a range of stagnation enthalpies corresponding to flight Mach number variations of  $\sim\pm 0.5$ . Condition 6d does not represent a true achievable flight condition because, although the value of  $M_0$  listed is consistent with the stagnation enthalpy, it is not consistent with the isolator entrance Mach number. For this reason, a dynamic pressure is not quoted.

## EXPERIMENTAL RESULTS

A total of thirty-nine successful, full-duration, fueled tests were conducted at the nominal Mach 6 test condition. The first thirty-one of these were conducted with ethylene and the final 8 tests were conducted with the surrogate fuel mixture. Table 2 shows the number of tests conducted with each fuel injector configuration and the chronological order in which they were performed. Recall that in the 4x4 injector configuration, the injection was not sonic, but injection was sonic for the 2x2 configurations. Also recall that the "C" denotes the addition of the choked orifices upstream of the fuel injector ports to ensure equal lateral fuel distribution for the unchoked 4x4 injector configuration.

Table 2 Summary of fuel types and injector configurations tested.

| Fuel Type | Fuel Injector Configuration | # tests |
|-----------|-----------------------------|---------|
| Ethylene  | 4 x 4                       | 7       |
|           | 2 x 2 P-I/S-I               | 2       |
|           | 2 x 2 P-I/S-O               | 19      |
|           | 4 x 4 C                     | 3       |
| Surrogate | 4 x 4 C                     | 8       |

### INFLOW

It is important to assess the inflow to the combustor prior to interpreting fueled test results. The isolator wall pressures can be inspected to determine, to some level, the quality of the combustor inflow. Mach 6 test results showed unexpected isolator wall pressure distributions. The expected surface pressure distribution for a tare (no fuel) condition was a near constant pressure along the 8-inch length of the constant area isolator equal to the expected one-dimensional isolator inflow pressure of approximately 11 psia (for a plenum pressure of  $P_{t,pl}=212$  psia). Figure 10 shows bodyside (BS) and cowlside (CS) centerline tare pressure distributions from a representative Mach 6 test. (*Note: In all the pressure distributions presented in this report, the pressures have been scaled to the baseline facility stagnation pressure of 212 psia, to account for run-to-run and during-run variations in facility stagnation pressure.*). The most notable feature is the difference between the BS and CS wall pressures at the isolator entrance, and the drop in pressure on both BS and CS at the 2.5 inch axial station. Quarter span 3D CFD solutions using the as-designed flowpath did not indicate any such pressure variations. After phase I testing with the Mach 6 facility nozzle was completed, a mold of the inner surfaces was made from the nozzle throat through the first isolator section. From inspection of this mold, aft facing steps on both the BS and CS with heights greater than 0.010 inches were identified at the nozzle/isolator interface. The nozzle exit plane CFD solution indicated that the sub-sonic boundary layer was very thin at this

interface (~ 0.003"). It is speculated that a streamline shift is occurring at this junction, which is generating a Prandtl-Meyer (P-M) expansion wave, followed by an immediate recompression shockwave. At the Mach 6 inflow condition, a Mach wave calculation indicates that the P-M wave angle would impact at approximately the 2.5 inch axial station. A higher fidelity CFD analysis is underway to verify this result, and bring closure to the suspect non-uniformity in the centerline static wall pressures in the isolator section.

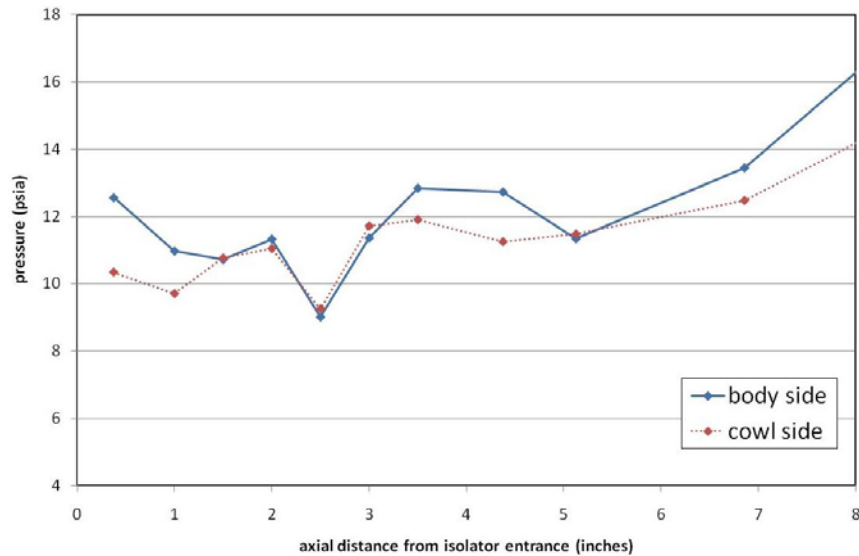


Figure 10. Isolator centerline axial pressure distribution.

## FUELED RESULTS / OPERABILITY

This section presents fueled test results covering a range of test conditions and primary to secondary fuel splits. Unless otherwise noted, all results shown are for the surrogate fuel in the baseline 4x4 C configuration, but comparisons with ethylene and with other fuel injection configurations are also presented.

One of the HDCR test objectives was to identify fuel splits that would provide stable operation for ignition and for transition from dual-mode to scramjet-mode, both with margin for uncertainties. As a metric for establishing an acceptable maximum fuel equivalence ratio operability limit, it was decided that if the isolator margin (defined as the length of isolator ahead of the pre-combustion shock pressure rise, divided by the total isolator length) was reduced to less than 50%, that the operating condition would be unacceptable for flight. This margin was deemed necessary to account for uncertainties including effects resulting from the differences between ground test and flight.

A typical fuel schedule, shown in Figure 11, consisted of stepping the primary and secondary equivalence ratio ( $\phi$ ) values to an initial fuel split for ignition and then holding either the primary or secondary  $\phi$  constant while the other was increased over a range of values (with dwell times of about 2 seconds at each fuel split to obtain steady data). In this way it was possible to investigate the sensitivity of the engine operation to fueling from each injection station independently.

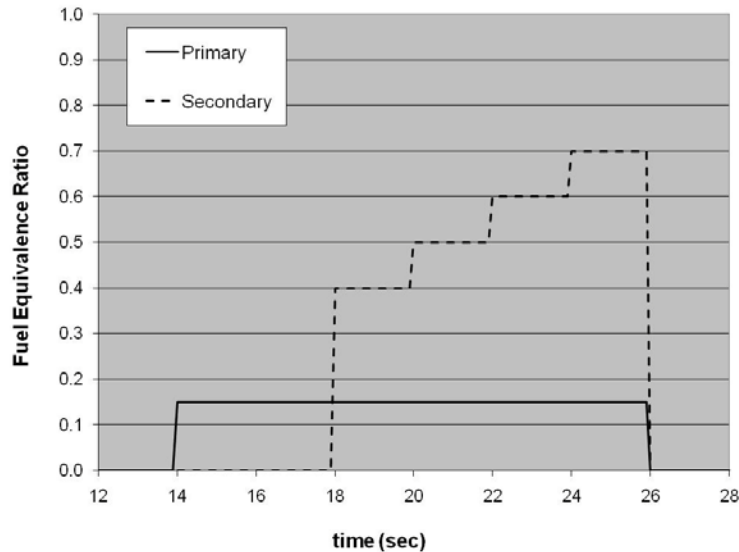


Figure 11. Typical HDCR fuel schedule.

Initial testing at the baseline condition (simulated  $M_o=5.84$ ,  $q_o=1060$  psf ) with ethylene in the 4x4 configuration showed that engine operation was very sensitive to the primary fuel level. A relatively lower than expected primary  $\phi$  ( $\phi(\text{pri})$ ) of less than 0.3 was necessary to maintain reasonable isolator margin and a  $\phi$  of 0.5 from the primary alone resulted in zero isolator margin. For this reason, and because ethylene and the surrogate fuel demonstrated similar operation (to be shown later in this section) no tests of the surrogate fuel at  $\phi(\text{pri}) > 0.25$  were conducted at Mach 5.84 enthalpy. Figure 12 shows tare and fueled pressure distributions, for both body and cowl sides at the baseline Mach 6 condition (simulated  $M_o=5.84$ ,  $q_o=1060$  psf) with the surrogate fuel in the 4x4 C configuration. The ignition fuel split of  $\phi(\text{pri}/\text{sec}) = 0.15/.40$  readily ignited with 100% isolator margin, as shown, and was stable. The three fueled pressure distributions show the sensitivity of the engine operation to increasing secondary  $\phi$  from 0.4 to 0.5, and to 0.6. None of the fuel splits shown violate the 50% isolator margin limit. As the secondary  $\phi$  ( $\phi(\text{sec})$ ) was incrementally increased, an incremental rise in the isolator, cavity, and combustor wall pressures occurred. A final observation is that the body and cowl sides show very similar pressure distributions, as expected for this symmetric flowpath. For this reason, the remaining plots show only body-side for simplicity.

Figure 13 shows results obtained when  $\phi(\text{sec})$  was increased to 0.7 in relation to those shown Figure 12, but now showing bodyside only. Increasing  $\phi(\text{sec})$  from 0.6 to 0.7 at  $\phi(\text{pri})$  of 0.15 resulted in 38% isolator margin, excessively high isolator pressures and a drastic drop in pressure downstream of the cavity.

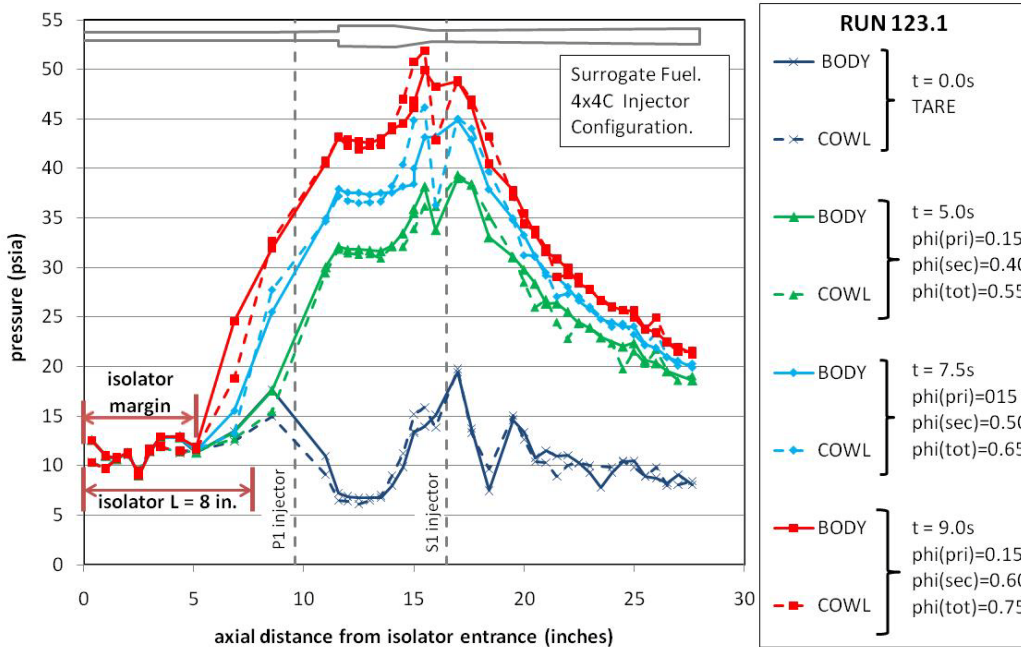


Figure 12. BS and CS Centerline Pressures for Mach 5.84 Operation: Sensitivity to Secondary Fueling.

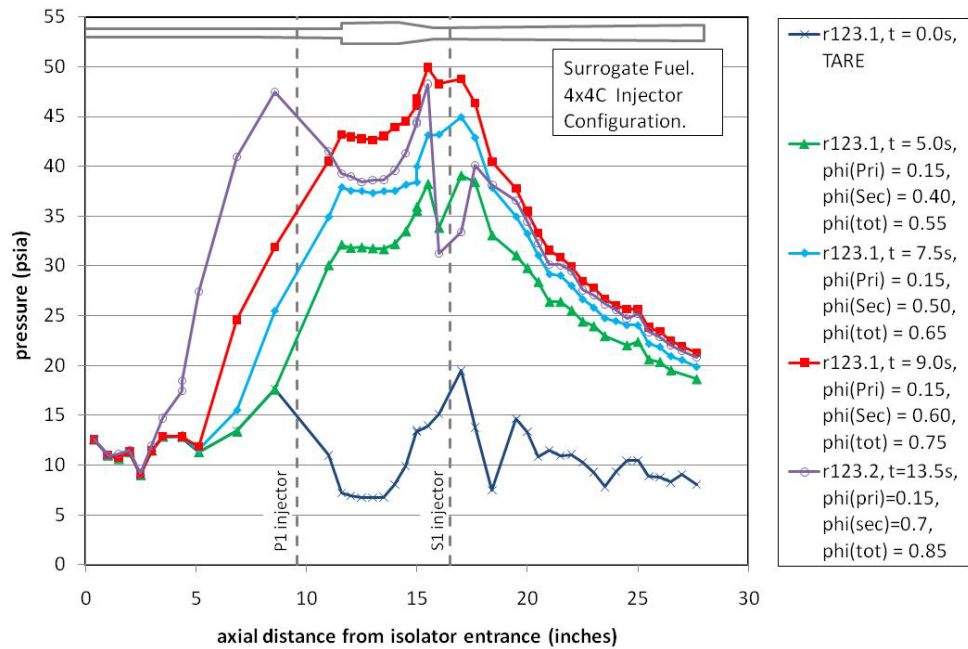


Figure 13. BS Centerline Pressures for Mach 5.84 Operation: Sensitivity to Secondary Fueling.

Testing was also conducted at the baseline condition at a higher primary phi of 0.25 with secondary phi's of 0.4 and 0.5. The resulting pressure distributions are shown in Figure 14, with selected distributions from Figure 13 included for comparison. Figure 14 allows comparison of results obtained with different fuel splits, but at the same total phi. For the same total phi values, at both 0.65 and 0.75, shifting more of the fuel forward from secondary to primary resulted in noticeably lower cavity and peak combustor pressures (and presumably lower performance), but did not affect the isolator margin. Figure 14 also serves to summarize the full range of total phi's and fuel splits over which acceptable operation was achieved. However, the fuel split of  $\phi(\text{pri/sec})=0.15/0.60$  proved not to be a stable operating point as it sometimes demonstrated operation similar to that shown for the 0.15/0.70 fuel split, as shown in Figure 14. The two modes were demonstrated during steady 2 sec dwells at this fuel split, as well as in repeat tests at this fuel split. Because of the instability at  $\phi(\text{pri/sec})=0.15/0.60$ , it was eliminated as a candidate fuel split for flight. All other fuel splits demonstrated repeatability and the fuel split of  $\phi(\text{pri/sec})=0.15/0.5$  was selected as a baseline candidate fuel split for flight.

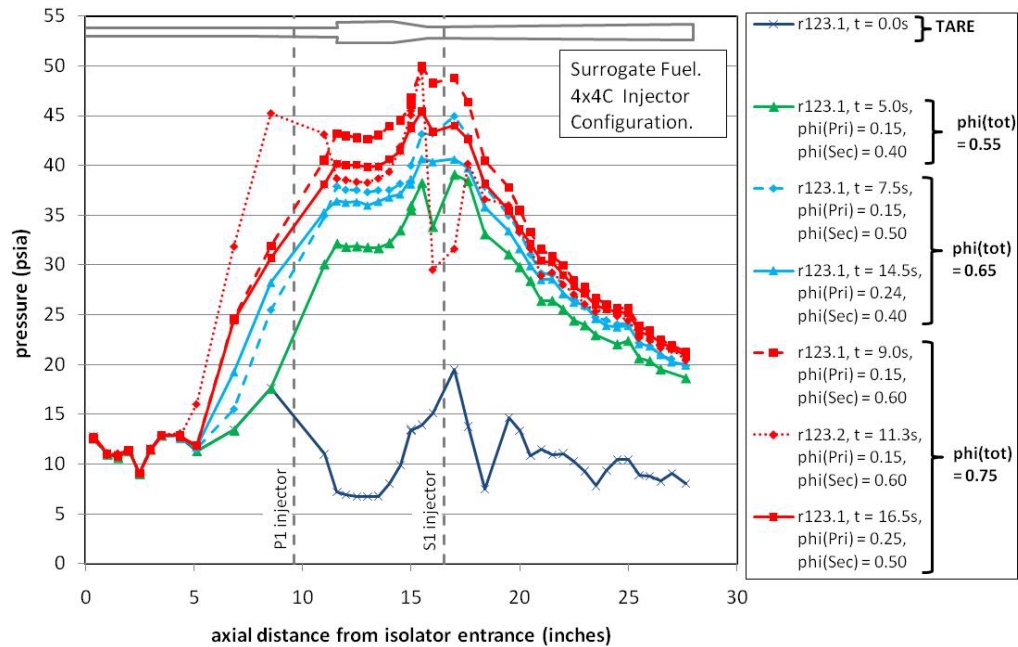


Figure 14. BS centerline pressures for Mach 5.84 operation over a range of fuel splits.

- Pressure Sensitivity

Mach 5.84 surrogate-fueled tests in the 4x4 C injector configuration were conducted at 30% increased facility plenum pressure/dynamic pressure compared to the baseline (test condition 6b from Table 1) to investigate the sensitivity of engine operation to flight dynamic pressure. Results from two different tests conducted at facility plenum pressures of 212 and 275 psia, respectively, but using nearly identical fuel equivalence ratio schedules, are shown in Figure 15. The fuel splits obtained were  $\phi(\text{pri/sec})=0.15/0.4$ ,  $0.15/0.5$ , and  $0.15/0.6$ . All pressures have been scaled to the baseline facility stagnation pressure of 212 psia. Results show that the pressure distributions scale well and confirm that



operability and performance are not functions of inflow pressure (i.e. flight dynamic pressure), over the range investigated ( $q_0=1060$  to  $1370$  psf).

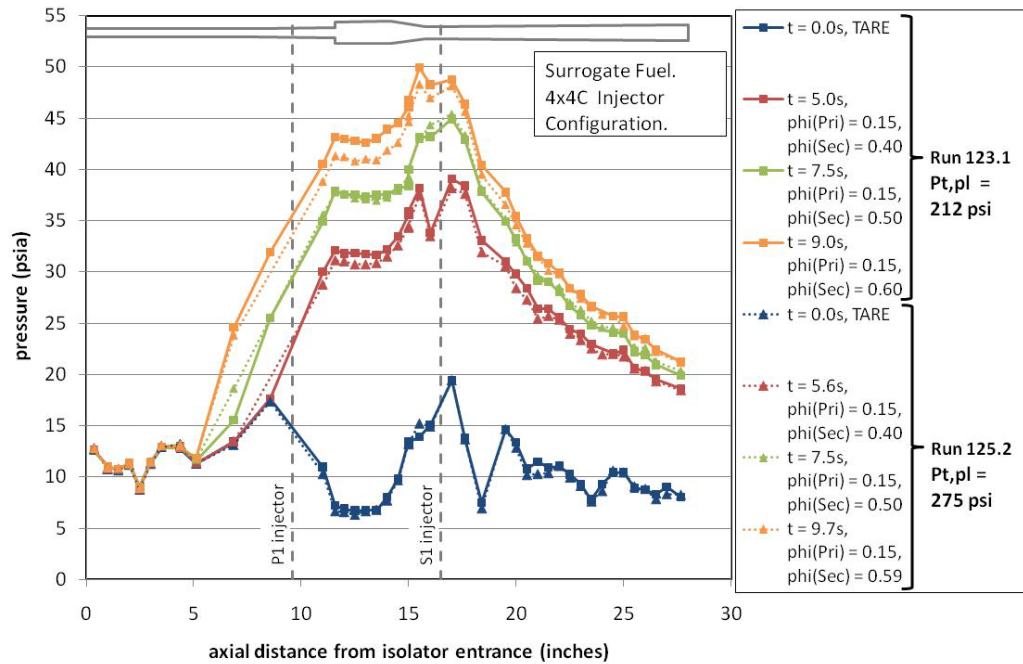


Figure 15. Mach 5.84 comparison of operation with increased facility pressure.

- Enthalpy Sensitivity

Surrogate-fueled tests were also conducted at Mach 6.5 enthalpy (test condition 6d from Table 1) in the 4x4 C fuel injector configuration. Although not representative of any specific flight condition, these tests served to demonstrate the effect of stagnation enthalpy on the combustion characteristics and operability. The fuel splits tested at Mach 6.5 enthalpy were primary phi values of 0.2 to 0.5 at a fixed secondary phi of 0.5, as well as secondary phi values of 0.3 to 0.6 at a fixed primary phi of 0.4. Pressure distributions at the extremes of these phi ranges are shown in Figure 16. Compared to results at Mach 5.84 (see Figure 14), results at Mach 6.5 enthalpy show less pressure rise in the combustor, as expected, along with less combustor-isolator interaction for the same total phi. (Compare  $\phi(\text{tot})=0.7$  at Mach 6.5 with  $\phi(\text{tot})=0.65$  and  $0.75$  at Mach 5.84). The baseline fuel split selected for the Mach 6.5 enthalpy condition was  $\phi(\text{pri}/\text{sec}) = 0.4/0.6$ .

- Fuel Type Sensitivity

Figure 17 is a comparison of the results with ethylene and the surrogate fuel mixture at the same nominal inflow condition ( $M_0=5.84$ ,  $q_0=1060$  psf), same injector configuration (4x4 C) and nearly identical fuel splits. The tare pressure distributions for both runs are comparable. For the  $\phi(\text{pri}/\text{sec}) = 0.2/0.4$  and  $0.2/0.5$  fuel splits, the different fuels show similar combustion results, especially at the  $\phi(\text{pri}/\text{sec})=0.2/0.4$  split. The pre-combustion pressure rise anchors at the same axial location for both fuels.

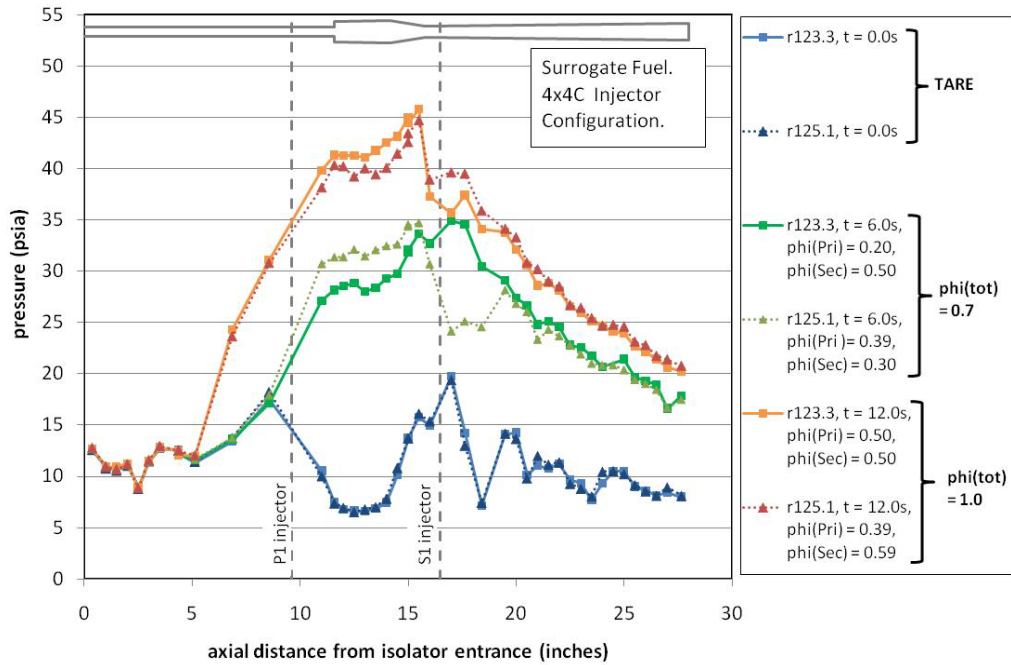


Figure 16. Operations at Mach 6.5 enthalpy, over a range of fuel splits.

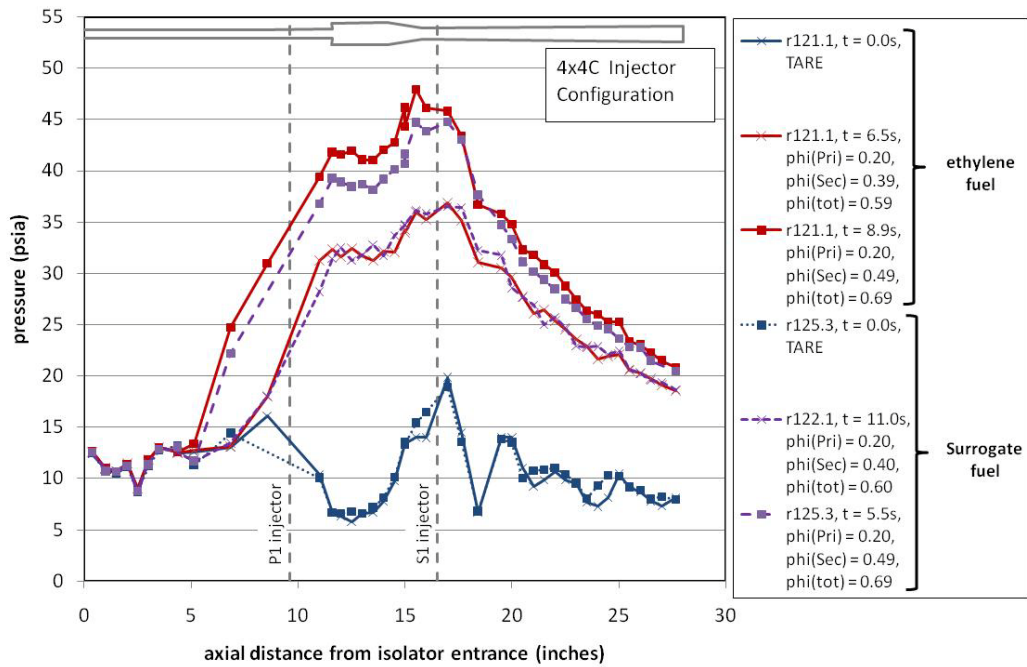


Figure 17. Sensitivity of HDCR dual-mode operations to fuel type.

- Fuel Injector Configuration Comparisons

Of the various fuel injector configurations tested (see Table 2), the addition of the choked orifices in the 4x4 configuration to ensure equal lateral fuel distribution at each station proved to have no significant effect. However, the 2x2 injector configurations, tested to explore the effect of penetration and mixing on flowpath operation, had the effect of increasing the isolator margin relative to the 4x4 configuration. This is demonstrated in Figure 18, which shows a comparison of both the 2x2 P-I/S-I, and the 2x2 P-I/S-O configurations with the 4x4 C configuration. All results are for the baseline Mach 5.84 condition at the same fuel split of  $\phi(\text{pri}/\text{sec})=0.30/0.50$ , with ethylene. (The comparison can only be shown for ethylene fuel because surrogate fuel was only tested in the 4x4C configuration and possible differences due to fuel type might cloud the comparison.). In the 4x4 C configuration at this fuel split, the combustion-induced pressure rise advanced unacceptably far forward (approximately 20% isolator margin) and there was a drop in pressure for a short distance, just downstream of the cavity. The first 2x2 configuration tested was the 2x2 P-I/S-I (only the two inner injection holes used at both the primary and secondary stations), and although isolator margin was increased compared to the 4x4 configuration, the peak pressure (in the cavity) was lower, and lower pressures downstream of the cavity indicated poor mixing/weak combustion. It was suspected that an improvement in secondary fuel mixing and burning could be achieved by re-configuring the secondary injectors to use only the outer two holes (a 2x2-O configuration). As shown in Figure 18, the 2x2 P-I/S-O indeed resulted in improved downstream combustion, compared to the 2x2 P-I/S-I configuration (as well the 4x4C configuration), with some loss in isolator margin compared to the 2x2 P-I/S-I configuration, but still within the established 50% limit. Nearly identical results were obtained when comparing the 4x4C and 2x2 P-I/S-O at the same total  $\phi$  of 0.8, but at a fuel split of  $\phi(\text{pri}/\text{sec})=0.2/0.6$ . However, at reduced total  $\phi$  of 0.7, and a fuel split of  $\phi(\text{pri}/\text{sec})=0.2/0.5$ , the 2x2 P-I/S-O demonstrated two different modes of operation, as shown in Figure 19. In this comparison, one mode of the 2x2 operation is very similar to the 4x4C operation, while the other mode yielded less combustion pressure rise and increased isolator margin.

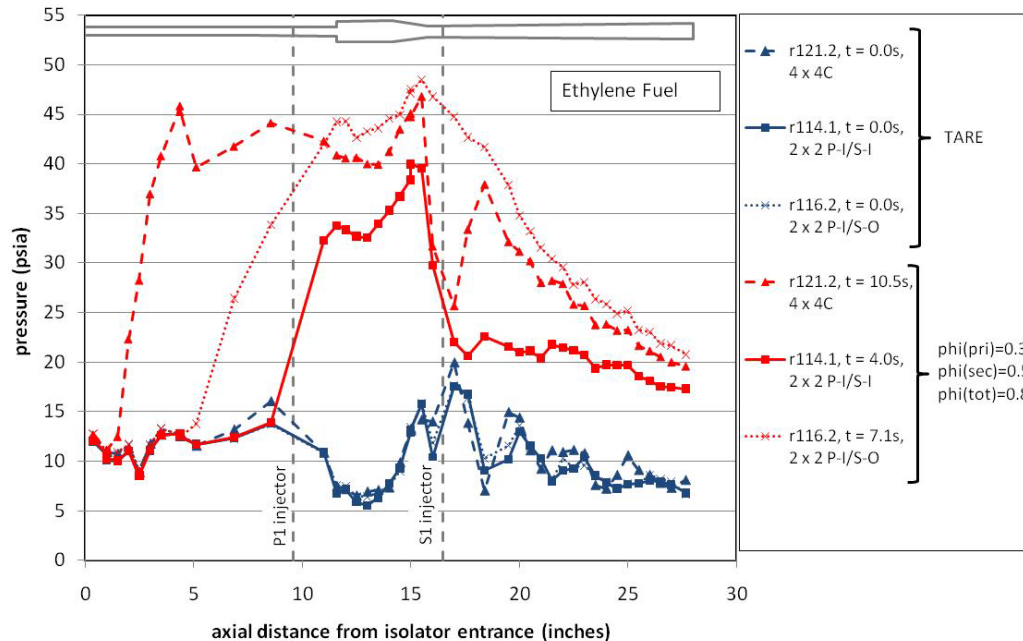


Figure 18. Comparison of the 2x2 and 4x4C injector configurations at M5.84 at  $\phi(\text{tot})=0.8$

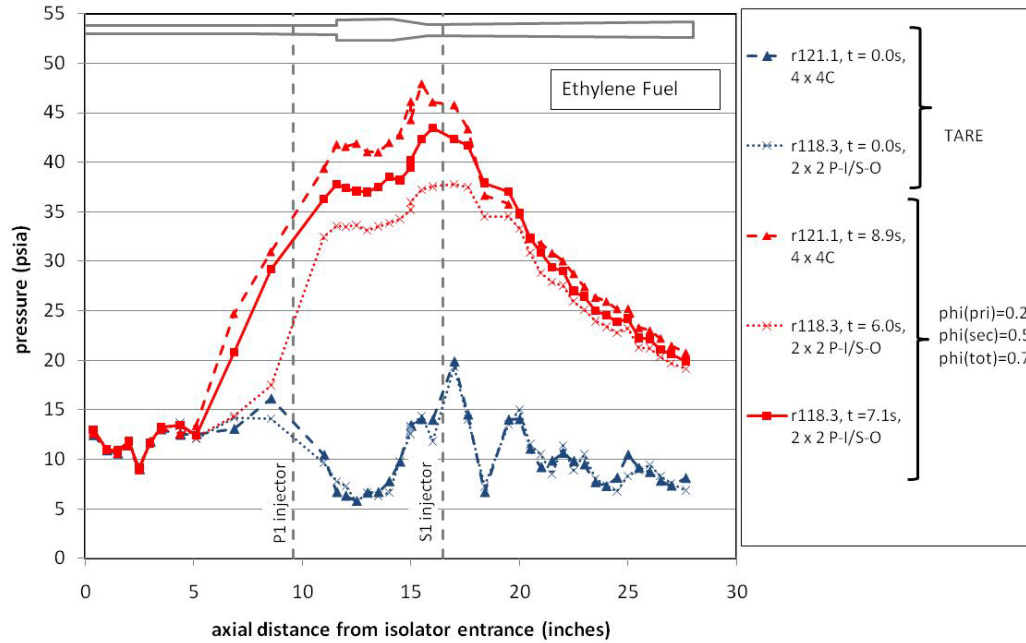


Figure 19. Comparison of the 2x2 and 4x4C injector configurations at M5.84 at  $\phi(\text{tot})=0.7$

- Ignition Assistance Testing

Successful ignition without spark ignitors was demonstrated with both the ethylene and surrogate fuel at Mach 5.84 conditions. The fuel splits at ignition were repeats of previous runs. The resulting pressure profiles were nearly identical for the same fuel splits and remained stable, indicating that flameholding after ignition is not an issue in the dual-mode operation.

- Thermal Data

The measured heat fluxes for the Mach 5.84, tare and 0.15/0.6 primary to secondary fuel split, are shown in Figure 19. The heat flux gauge at the 3" axial station showed no change between the tare and fueled portion of the test. However, the cavity and combustor heat flux gauges showed a substantial increase in heat flux when combustion was present.

The wall temperatures measured for the Mach 5.84 tare and 0.15/0.6 primary to secondary fuel split, are shown in Figure 20. Much like the heat flux measurements, little temperature rise was notable at the 3" axial station thermocouple. The symbols having a white fill are those on the body side of the flowpath that still have a TBC on their exposure surface. Note how much lower they are than the exposed thermocouples at the same axial station at tare and after a combustion duration of nearly six seconds. Although not shown in this plot, backside temperatures were also measured at several stations to extrapolate heat flux and compare to heat flux gauge measurements. The technique for determination of heat flux from these measurements is described in detail in reference 12.

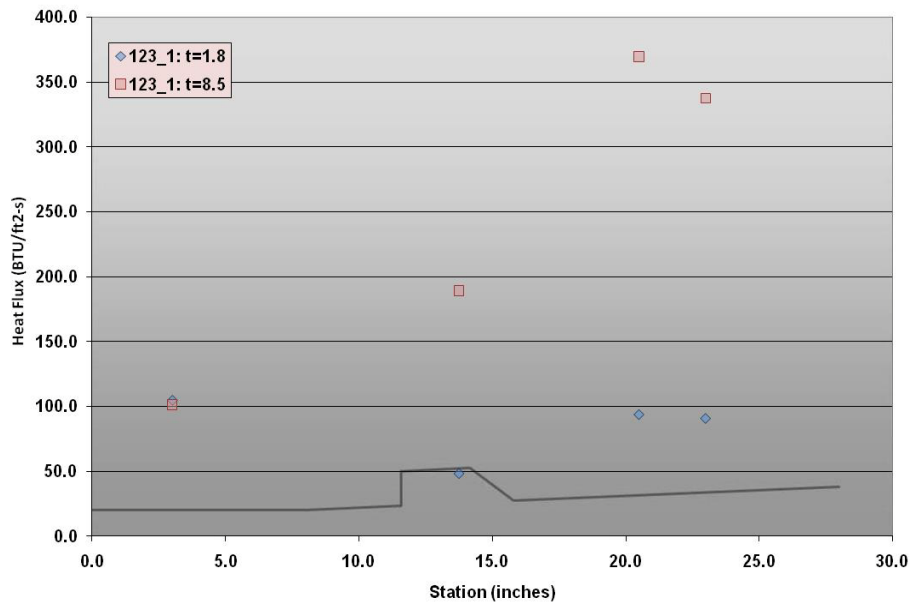


Figure 20. Measured Heat Flux, M5.84, tare (run 123.1: t=1.8) vs. 0.15/0.6 fuel split (run 123.1: t=8.5).

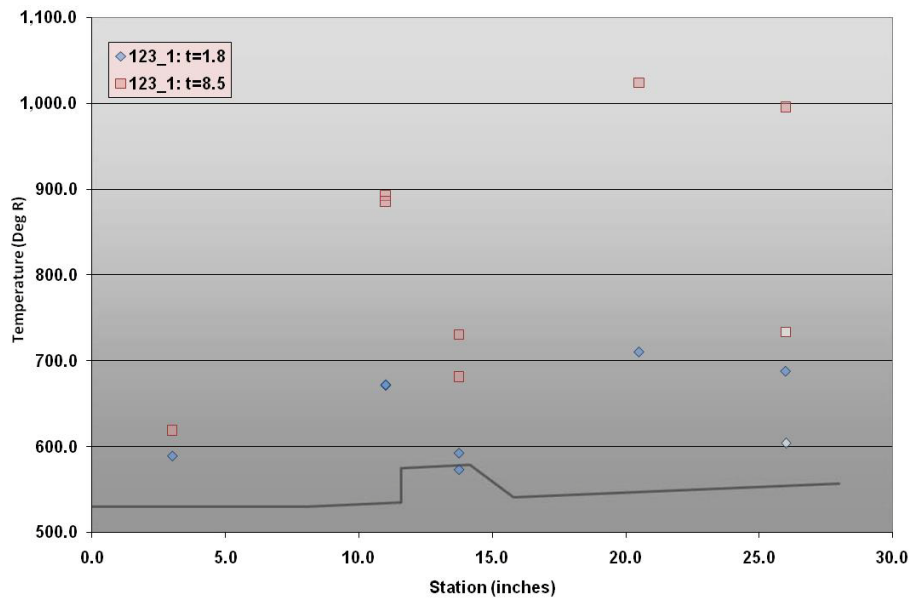


Figure 21. Measured Wall Temperatures, M5.84, tare (run 123.1: t=1.8) vs. 0.15/0.6 fuel split (run 123.1: t=8.5).

## TEST SUMMARY

A total of 39 fueled tests have been conducted in this first phase of Mach 6 testing. Of these, 31 were fueled by ethylene, instead of the surrogate mixture. The parameters that were exercised in this first phase of testing consisted of total enthalpy, total pressure, fuel splits, fuel injector configuration, ignition assistance, and fuel type. A chart summarizing the key parametric testing elements is shown below in Table 3. The table is set up in a matrix of the “as tested” primary versus secondary equivalence ratios for a number of enthalpy and total pressure test conditions for the Mach 6 test series. The content of the matrices is filled with rating information. For those fuel splits that successfully operated with an isolator margin greater than 50%, the space is filled in with green, whereas those having less than 50% margin are indicated with the red fill. Yellow fill indicate test points that had both failed and successful operations. Each box has a number in it that correlates to the injector arrangement that was tested. The numbers indicated by the key dictate the number of bodyside and cowside injectors (ex – 2x2 means two BS and two CS primary by two BS and two CS secondary). Those cases having values enclosed in parenthesis are cases with the total pressure above the nominal (Pt,pl=275 and 318 psia). Note that only steady-state condition data points are reported in this table.

**Table 3. Summary of M6 runs, parametrics exercised, and successes.**

| Enthalpy = 719 BTU/lbm           |           |               | ~ Mach = 5.84                  | Secondary Fuel Equivalence Ratio |         |     |         |         |         |         |         |   |   |   |   |
|----------------------------------|-----------|---------------|--------------------------------|----------------------------------|---------|-----|---------|---------|---------|---------|---------|---|---|---|---|
| Total Pressure = 212 psia        |           |               | Primary Fuel Equivalence Ratio | 0                                | 0.25    | 0.3 | 0.4     | 0.5     | 0.6     | 0.7     | 0.8     |   |   |   |   |
| Dyn. Pressure = 1060 psf         |           |               |                                | 0.10                             |         |     |         |         |         |         |         |   |   |   |   |
| Key: Fuel Injectors              |           |               |                                | 0.15                             |         | 5   |         |         | 5       |         | 5       | 5 |   | 5 | 5 |
| 1                                | C2H4      | 4x4           |                                | 0.20                             | 3       | 4   |         | 3       | 4       | 5       | 3       | 4 | 5 | 3 | 4 |
| 2                                | C2H4      | 2 x 2 P-I/S-I |                                | 0.25                             | 1       |     | 1       |         | 5       | 1       | 5       |   |   |   |   |
| 3                                | C2H4      | 2 x 2 P-I/S-O |                                | 0.30                             | 2       | 3   |         |         | 2       | 3       | 4       | 3 |   | 3 |   |
| 4                                | C2H4      | 4 x 4 C       |                                | 0.40                             | 2       |     |         |         |         | 3       | 4       |   |   |   |   |
| 5                                | Surrogate | 4 x 4 C       |                                | 0.50                             | 1       | 2   | 1       | 1       |         | 1       | 3       |   |   |   |   |
| = Margin > 50%                   |           |               |                                | 0.60                             |         |     |         |         |         |         |         |   |   |   |   |
| = Both                           |           |               |                                | 0.70                             |         |     |         |         |         |         |         |   |   |   |   |
| = Margin < 50%                   |           |               | 0.80                           |                                  |         |     |         |         |         |         |         |   |   |   |   |
| Enthalpy = 719 BTU/lbm           |           |               | ~ Mach = 5.84                  | Secondary Fuel Equivalence Ratio |         |     |         |         |         |         |         |   |   |   |   |
| Total Pressure = (275, 318) psia |           |               | Primary Fuel Equivalence Ratio | 0                                | 0.2     | 0.3 | 0.4     | 0.5     | 0.6     | 0.7     | 0.8     |   |   |   |   |
| Dyn. Pressure = 1370, 1575 psf   |           |               |                                | 0.10                             |         |     |         |         |         |         |         |   |   |   |   |
| Key: Fuel Injectors              |           |               |                                | 0.15                             |         |     | 5 (275) | 5 (275) | 5 (275) |         |         |   |   |   |   |
| 1                                | C2H4      | 4x4           |                                | 0.20                             |         |     |         |         |         |         |         |   |   |   |   |
| 2                                | C2H4      | 2 x 2 P-I/S-I |                                | 0.25                             |         |     |         |         |         |         |         |   |   |   |   |
| 3                                | C2H4      | 2 x 2 P-I/S-O |                                | 0.30                             | 3 (318) |     |         |         | 3 (318) | 3 (318) | 3 (318) |   |   |   |   |
| 4                                | C2H4      | 4 x 4 C       |                                | 0.40                             |         |     |         |         |         |         |         |   |   |   |   |
| 5                                | Surrogate | 4 x 4 C       |                                | 0.50                             |         |     |         |         |         |         |         |   |   |   |   |
| = Margin > 50%                   |           |               |                                | 0.60                             |         |     |         |         |         |         |         |   |   |   |   |
| = Both                           |           |               |                                | 0.70                             |         |     |         |         |         |         |         |   |   |   |   |
| = Margin < 50%                   |           |               | 0.80                           |                                  |         |     |         |         |         |         |         |   |   |   |   |
| Enthalpy = 873 BTU/lbm           |           |               | ~ Mach = 6.5                   | Secondary Fuel Equivalence Ratio |         |     |         |         |         |         |         |   |   |   |   |
| Total Pressure = 212 psia        |           |               | Primary Fuel Equivalence Ratio | 0                                | 0.2     | 0.3 | 0.4     | 0.5     | 0.6     | 0.7     | 0.8     |   |   |   |   |
| Dyn. Pressure = N/A psf          |           |               |                                | 0.10                             |         |     |         |         |         |         |         |   |   |   |   |
| Key: Fuel Injectors              |           |               |                                | 0.15                             |         |     |         |         |         |         |         |   |   |   |   |
| 1                                | C2H4      | 4x4           |                                | 0.20                             | 3       |     |         | 3       |         | 3       | 5       | 3 |   | 3 |   |
| 2                                | C2H4      | 2 x 2 P-I/S-I |                                | 0.25                             |         |     |         |         |         |         |         |   |   |   |   |
| 3                                | C2H4      | 2 x 2 P-I/S-O |                                | 0.30                             | 3       |     |         |         |         | 3       | 5       | 3 |   | 3 |   |
| 4                                | C2H4      | 4 x 4 C       |                                | 0.40                             | 3       | 5   | 3       | 3       | 5       | 3       | 5       | 3 | 5 |   |   |
| 5                                | Surrogate | 4 x 4 C       |                                | 0.50                             |         |     |         |         |         | 3       | 5       |   |   |   |   |
| = Margin > 50%                   |           |               |                                | 0.60                             | 3       |     |         | 3       |         |         |         |   |   |   |   |
| = Both                           |           |               |                                | 0.70                             |         |     |         |         |         |         |         |   |   |   |   |
| = Margin < 50%                   |           |               | 0.80                           |                                  |         |     |         |         |         |         |         |   |   |   |   |

## CONCLUSIONS

To assure the success of the HIFiRE Flight 2 experiment, a ground test program is being conducted with a direct-connect test rig (HDCR) that is nearly an exact duplicate of the flight test component flowpath features. The goals of the HDCR ground test experiment are to 1) to verify that the isolator/combustor portion of the HIFiRE flowpath design demonstrates satisfactory operability with margin, using the surrogate fuel, spanning the engine transition from dual-mode to scramjet operation, across the flight test trajectory window and 2) to provide data to support analytical tools verification.

The results from the first phase of the HDCR verify that the flowpath design, both inner mold lines and injector sites, will support the dual-mode operations in flight. From the dual-mode test results, a fuel equivalence ratio range of 0.15 – 0.25 from the primary injection site, at the lowest enthalpy expected for any flight operations ( $M=5.84$ ), provides good operability. Running concurrently with the primary, the secondary injection site can support an equivalence ratio range of operability of 0.4 – 0.6, providing a baseline fuel schedule at ignition. From the results, a target fuel equivalence ratio split of primary to secondary 0.15/0.4 has been baselined for the 4x4 fuel injector arrangement at Mach 5.84. Increasing the enthalpy during dual-mode to Mach 6.5, improves the range of operability. At the Mach 6.5 condition, the primary equivalence ratio operability range increased to 0.2 – 0.5 and the secondary range changed to 0.3 – 0.6. From these results, the Mach 6.5 fuel injection equivalence ratio split, primary to secondary, baselined for the flight experiment is 0.4/0.6. Throughout the dual-mode testing, the combustion was strong and stable with these fuel splits, for this flowpath design. Ignition and flameholding without spark plug assistance was also demonstrated. Finally, the isolator margin was insensitive to the type of fuel used (ethylene or the surrogate fuel mixture). The completion of this testing phase provides to scramjet researchers a comprehensive data set of hydrocarbon fueled dual-mode combustion data with which to verify analytical prediction tools.

## FUTURE PLANS

Mach 8 testing is underway. A limited number of surrogate-fueled tests have been completed with both a 4x4 fuel injector configuration, as well as, a 2x2 fuel injector configuration. Finalized data sets are not available at the time of this writing. The focus of the Mach 8 testing is to identify fuel splits that yield acceptable operability in pure scramjet mode. If schedule is available, ethylene will be tested, but it is not required due to the similar behavior exhibited in the Mach 6 testing. Other important results from the Mach 8 testing include auto-ignition and flameholding.

In addition to the hardware testing, 3D CFD performance prediction tools will be exercised against the test conditions to assess, and verify present capability. Studies of the Mach 6 results are already underway, and preliminary results show good agreement, but more work is necessary to tune the flow physics models.

## ACKNOWLEDGEMENTS

The authors would like to thank Mark Gruber and Kevin Jackson at AFRL for their assistance.

## REFERENCES

1. Dolvin, Doug J., "*Hypersonic International Flight Research Experimentation*", AIAA/DLR/DGLR 16<sup>th</sup> International Space Planes and Hypersonic Systems and Technologies Conference, Bremen, Germany, October, 2009.
2. Jackson, Kevin M., et al, "*HIFiRE F2 Scramjet Experiment Overview*", 55th JANNAF Propulsion Meeting, Newton, MA, May, 2008.
3. Pellett, G. L., Vaden, S. N., and Wilson, L. G., "*Opposed Jet Burner Extinction Limits: Simple Mixed Hydrocarbon Fuels vs. Air*", AIAA Paper 2007-5664, 2007.
4. Smart, M. K., Hass, N. E., and Paull, A., "Flight Data Analysis of the HYSHOT 2 Scramjet Flight Experiment", *AIAA Journal of Propulsion and Power*, Vol. 44, No. 10, October, 2006, pg. 2366-2375
5. Ferlemann, Paul G., "*Forebody and Inlet Design for the HIFiRE F2 Flight Test*", 55th JANNAF Propulsion Meeting, Newton, MA, May, 2008.
6. Lai, H. and Thomas, S., "*Numerical Study of Contaminant Effects on Combustion of Hydrogen, Ethane and Methane in Air*", AIAA Paper 95-6097, 1995.
7. Cabell, K. F. and Rock, K.E., "*A Finite Rate Chemical Analysis of Nitric Oxide Flow Contamination Effects on Scramjet Performance*", NASA TP-212159, May, 2003.
8. Pellett, G. L., Dawson, Lucy C., Vaden, Sarah. N., and Wilson, Lloyd. G., "*Nitric Oxide and Oxygen-Air Contamination Effects on Extinction Limits of Non-premixed Hydrocarbon-Air Flames for a HIFiRE Scramjet*", JANNAF 43<sup>rd</sup> CS / 31<sup>st</sup> APS / 25<sup>th</sup> PSHS Joint Subcommittee Meeting, December, 2009, La Jolla, CA.
9. Guy, R. W., Torrence, Marvin G., Sabol, Alexander P. and Mueller, James N., "*Operating Characteristics of the Langley Mach 7 Scramjet Test Facility*", NASA TM-81929, 1981.
10. Guy, R. Wayne, Rogers, R. Clayton, Puster, Richard L., Rock, Kenneth E. and Diskin, Glenn S., "*The NASA Langley Scramjet Test Complex*", AIAA Paper 96-3243, 1996.
11. Lemmon, E. W., Huber, M. L., McLindon, M. O., *REFPROP - Reference Fluid Thermodynamic and Transport Properties, NIST Standard Reference Database 23, Version 8.0, 2007.*
12. Gruber, M. R., Jackson, K. R., Jackson, T. A., and Liu, J., "*Hydrocarbon-Fueled Scramjet Combustor Flowpath Development for Mach 6-8 HIFiRE Flight Experiments*", 55th JANNAF Propulsion Meeting, Newton, MA, May, 2008.
13. Cuda, Vincent, and Hass, Neal, "Heat Flux and Wall Temperature Estimates for the NASA Langley HIFiRE Direct Connect Rig", JANNAF 43<sup>rd</sup> CS / 31<sup>st</sup> APS / 25<sup>th</sup> PSHS Joint Subcommittee Meeting, December,, 2009, La Jolla, CA.
14. Ferlemann, Paul G., "*HIFiRE 2 Forebody and Inlet Analysis at Nominal Conditions for the 9 Inch Capture Design*", Technical Note 09-531 (Contract # NNL07AA00B), NASA Langley Research Center, August, 2009.